Received: 3 August 2019 | Revised: 15 September 2019 | Accepted: 30 September 2019

DOI: 10.1002/rcm.8616

RESEARCH ARTICLE

WILEY Rapid Communications in Mass Spectrometry

Development of a relative quantification method for infrared matrix-assisted laser desorption electrospray ionization mass spectrometry imaging of *Arabidopsis* seedlings

M. Caleb Bagley[1] | Anna N. Stepanova[2,3] | Måns Ekelöf[1] | Jose M. Alonso[2,3] | David C. Muddiman[1,2,4]

[1] Department of Chemistry, FTMS Laboratory for Human Health Research, North Carolina State University, Raleigh, NC 27695, USA

[2] Department of Plant and Microbial Biology, North Carolina State University, Raleigh, NC 27695, USA

[3] Program in Genetics, North Carolina State University, Raleigh, NC 27695, USA

[4] Molecular Education, Technology, and Research Innovation Center (METRIC), North Carolina State University, Raleigh, NC 27695, USA

Correspondence
D. C. Muddiman, FTMS Laboratory for Human Health Research, Department of Chemistry, North Carolina State University, Raleigh, NC 27695, USA.
Email: dcmuddim@ncsu.edu

Funding information
National Institutes of Health, Grant/Award Numbers: R01GM087964 and T32GM008776; National Science Foundation, Grant/Award Numbers: 1444561, 1650139 and 1750006

Rationale: Mass spectrometry imaging of young seedlings is an invaluable tool in understanding how mutations affect metabolite accumulation in plant development. However, due to numerous biological considerations, established methods for the relative quantification of analytes using infrared matrix-assisted laser desorption electrospray ionization (IR-MALDESI) mass spectrometry imaging are not viable options. In this study, we report a method for the quantification of auxin-related compounds using stable-isotope-labelled (SIL) indole-3-acetic acid (IAA) doped into agarose substrate.

Methods: Wild-type *Arabidopsis thaliana* seedlings, *sur2* and *wei8 tar2* loss-of-function mutants, and *YUC1* gain-of-function line were grown for 3 days in the dark in standard growth medium. SIL-IAA was doped into a 1% low-melting-point agarose gel and seedlings were gently laid on top for IR-MALDESI imaging with Orbitrap mass spectrometry analysis. Relative quantification was performed post-acquisition by normalization of auxin-related compounds to SIL-IAA in the agarose. Amounts of auxin-related compounds were compared between genotypes to distinguish the effects of the mutations on the accumulation of indolic metabolites of interest.

Results: IAA added to agarose was found to remain stable, with repeatability and abundance features of IAA comparable with those of other compounds used in other methods for relative quantification in IR-MALDESI analyses. Indole-3-acetaldoxime was increased in *sur2* mutants compared with wild-type and other mutants. Other auxin-related metabolites were either below the limits of quantification or successfully quantified but showing little difference among mutants.

Conclusions: Agarose was shown to be an appropriate sampling surface for IR-MALDESI mass spectrometry imaging of *Arabidopsis* seedlings. SIL-IAA doping of agarose was demonstrated as a viable technique for relative quantification of metabolites in live seedlings or tissues with similar biological considerations.

1 | INTRODUCTION

Mass spectrometry imaging (MSI) has become a preferred method for exploring metabolic distributions in their native biological structures, as a more complete understanding of an organism's biochemistry can be achieved by visualizing spatial distributions of metabolic pathways.[1] There are many viable methods for MSI that vary in extraction, ionization, and analysis mechanisms.

One of the most commonly used imaging techniques is matrix-assisted laser desorption/ionization (MALDI) which operates by using an energy-absorbing matrix to generate ions from biomolecules.[2] It is a robust technique that can provide chemical specificity as well as high spatial resolution.[3] Nevertheless, it has some inherent disadvantages: it requires significant sample preparation, matrix peaks dominate the low *m/z* acquisition range, and it occurs under vacuum, although there have been methods developed to remedy some of these drawbacks.[4,5]

Since its inception, electrospray ionization (ESI) mass spectrometry (MS) has been the catalyst for much of the MS work studying the chemical diversity of complex biological samples by enabling analysis of small metabolites to large proteins.[6-8] Such analytical dexterity has made it an invaluable ionization technique used in a diverse array of MS methods, most notably as an interface for liquid chromatography MS. Desorption ESI is one ambient MSI method that harnesses the benefits of ESI. It extracts secondary ions from tissues by bombarding the tissue with charged solvent droplets produced by electrospray, which makes it a soft ionization method that does not require sample preparation to measure the breadth of metabolite diversity in the sample.[9]

Infrared matrix-assisted laser desorption electrospray ionization (IR-MALDESI) combines many of the benefits of both MALDI and ESI, while addressing several of the drawbacks associated with each.[10,11] Analogous to MALDI, it is a laser desorption technique, but it does not require the use of an organic acid matrix, similar to atmospheric-pressure MALDI.[4,12] However, it ionizes molecules in an ESI-like manner, which gives it greater range for measuring the inherent biology of a sample without matrix artifacts contaminating the low *m/z* range. The ionization mechanism is the same as in ESI, with a significant improvement being the relative ease of absolute quantification of metabolites in tissue due to the quantitative removal of a reproducible volume (voxel) of tissue at each location on the tissue. Fundamentally, IR-MALDESI ablates neutral material using a mid-IR laser ($\lambda = 2940$ nm), which resonantly excites the O—H stretching mode of water endogenous to the sample or exogenously applied as an ice matrix.[13] Molecules are desorbed largely as neutrals that partition into charged droplets produced by ESI and are subsequently ionized in an ESI-like fashion. The ions are then analyzed in a Q Exactive Plus mass spectrometer (Thermo Scientific, San Jose, CA, USA) with high-resolution accurate mass, which is the primary approach for putative metabolite identifications from complex samples in IR-MALDESI MSI. The instrument is fully synchronized with ion generation from each voxel of ablated tissue.[14] Previous studies have worked towards a better understanding of the mechanisms of IR-MALDESI[13-16] and to develop methods that provide the analytical thoroughness necessary to enable meaningful biological conclusions for the analysis of mammalian tissues.[17]

Recently IR-MALDESI has been applied to plant tissues, which have many different inherent sampling challenges from mammalian tissues.[18] IR-MALDESI has proved to be a highly effective method for the analysis of a diverse range of plant tissues.[19-21] Each of these experiments answered specific fundamental biological questions. Naturally, quantification is the next step towards providing plant metabolite analysis with the analytical rigor applied to other sample types.[17,22]

In the study reported here, we developed a method for relative quantification of *Arabidopsis thaliana* metabolites in dark-grown seedlings. There were numerous sample-specific considerations and challenges that had to be met before biological conclusions could be drawn. Eventually, relative quantification was achieved through normalization to a standard internal to the agarose sampling surface. This method provides the analytical rigor necessary to afford biological insights into live plant tissues, specifically, *Arabidopsis* seedlings. Furthermore, changes in key metabolites in the auxin pathway due to mutations were examined in dark-grown *Arabidopsis* seedlings while maintaining sample integrity.

2 | MATERIALS AND METHODS

2.1 | Growing *Arabidopsis thaliana* seedlings

All *Arabidopsis* lines employed in this study are in Columbia background: wild-type (WT) Col-0, *sur2*,[23] *wei8 tar2*,[24] and *YUC1* overexpression (ox).[25] Seeds were surface-sterilized for 10 min with 50% commercial bleach (spiked with Triton at one drop per 100 mL) and washed three to four times with sterile deionized water. Seeds were resuspended in sterile, pre-cooled 0.7% top low-melting-point agarose (60 µL per *ca* 100 seeds) and plated on the surface of an AT plate (1 × MS salts, 1% sucrose, pH 6.0 with 1 M KOH, 0.7% Difco bactoagar) sector, up to eight lines per plate. After stratifying the plated seeds at 4°C for 3 days, the plates were exposed to ambient light for 1–2 h, wrapped with aluminium foil, and incubated horizontally at 22°C in the dark for 3 days. The plates were unwrapped, and the individual seedlings were picked with fine-pointed forceps, laid on the surface of pre-cooled stable-isotope-labelled (SIL) indole-3-acetic acid (IAA)-supplemented agarose glass slides, and imaged immediately.

2.2 | SIL doping of agarose

IAA (Sigma-Aldrich, St Louis, MO, USA) was doped into agarose before SIL-IAA to ensure that agarose could be effectively analyzed. Phenyl-$^{13}C_6$, 99% SIL-IAA from Cambridge Isotope Laboratories Inc. (Tewksbury, MA, USA) was doped into HS molecular biology-grade agarose (Denville Scientific Inc., Swedesboro, NJ, USA). IAA and SIL-IAA peaks were identified and resolved to ensure normalization

was possible (Figure S1, supporting information). Both types of IAA were dissolved in 95% EtOH at 10 mM concentration and stored in the dark at 4°C. A 1% agarose solution was made using deionized water. A microwave oven was used to heat the agarose in a 15–50 mL Falcon tube (Fisher Scientific, Waltham, MA, USA) until boiling, to dissolve the agarose powder. As the agarose cooled to 45–50°C, the SIL-IAA was added to the solution for a concentration of 1 mM and the mix was poured onto a microscope slide (1 mL agarose per standard glass slide spread thinly using a pipette), allowed to solidify away from light and heat, and used on the same day.

2.3 | IR-MALDESI imaging source

The IR-MALDESI source has been described in depth elsewhere.[13,15] A mid-IR Opotek IR Opolette 2371 laser (Carlsbad, CA, USA) resonantly excited the O—H stretching mode of endogenous water in a dark-grown seedling at 2940 nm. The ESI plume was 50:50 MeOH:H_2O with 1 mM acetic acid (all: Optima®, Fisher Chemical, Fair Lawn, NJ, USA) at a flow rate of 1 µL/min. The QE Plus hybrid quadrupole–orbitrap mass spectrometer employed in this study was fully synchronized with ion generation from laser desorption of a given voxel.[14] The laser was fired with one pulse with a fixed injection time (IT) of 25 ms. The spot size for laser ablation was *ca* 100 µm and this was also used as the step size between shots, providing a spatial resolution of 100 µm. Lock masses (positive polarity: *m/z* 359.3156, 371.1012, 391.2843) were employed to achieve low parts per million (ppm) mass accuracy. Ions in the *m/z* 150–600 range were analyzed with 140 000 resolving power (FWHM, *m/z* 200). Glass slides covered with agarose were placed on a Peltier cooled stage, which was set to −2°C for the duration of experiments. The mounted stage was controlled in *XY* dimensions using a computer controller.

2.4 | Data acquisition and analysis

The sample images were acquired by moving each sample under the laser and mass spectrometer inlet while synchronizing laser firing and mass spectrometer data acquisition. In-house-built software was used to define the sampling area, control the imaging process, and save the metadata required for constructing the molecular images. Instrument RAW files were converted to mzML using MSConvert[26,27] and then from mzML to imzML using the mzMLConverter.[28] Image generation and further analysis were performed using MSiReader (version 1.01).[29,30]

3 | RESULTS AND DISCUSSION

3.1 | Auxin pathways and knockout mutations

The biosynthetic pathway for plant hormone auxin shares intermediates with the biosynthesis of a group of defense compounds known as indole glucosinolates (IGs). Figure 1 depicts the current view of the tryptophan-dependent auxin biosynthesis pathway and shows its connection with the IG branch of secondary metabolism. Loss-of-function mutants *wei8 tar2* and *sur2* inactivate auxin production and IG biosynthesis, respectively, and consequently lead to IAA deficiency versus excess synthesis. Loss-of-tryptophan aminotransferases WEI8 and TAR2, the key enzymes in the indole-3-pyruvic acid (IPyA) route of auxin synthesis, are characterized by reduction in the levels of both IPyA and IAA.[24] Loss of the cytochrome P450 SUR2, an enzyme that channels indole-3-acetaldoxime (IAOx), a shared intermediate between the auxin and the IG biosynthetic pathways, into the production of IGs, is accompanied by IAOx hyperaccumulation,[23] with some of IAOx re-routed to the biosynthesis of IAA. Finally, gain-of-function of *YUC1*, a gene that encodes a rate-limiting flavin-containing monooxygenase in the IPyA branch of auxin biosynthesis, enhances the flow of metabolites through the IPyA route by increasing *YUC1* transcript levels and thus also leads to auxin overproduction.[25] In this work, we interrogated the following metabolites: tryptophan (Trp), IAOx, indole-3-acetamide (IAM), indole-3-acetonitrile (IAN), IGs, IPyA, indole-3-butyric acid (IBA), arginine (Arg), sucrose, and IAA (Figure S2, supporting information).

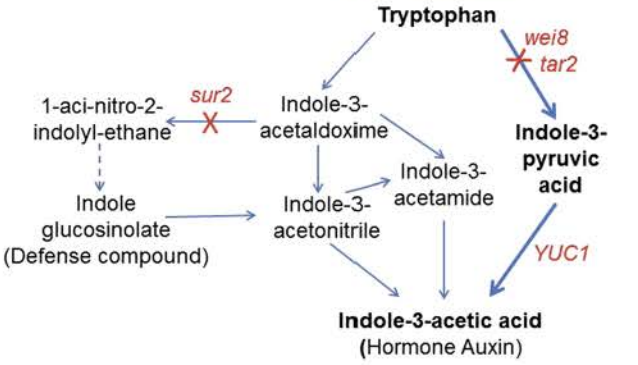

FIGURE 1 A model of interconnected auxin biosynthesis and indole glucosinolate biosynthesis pathways in *Arabidopsis*. Amino acid tryptophan is converted into plant hormone auxin, indole-3-acetic acid, predominantly via the indole-3-pyruvic acid route (bold), but other putative routes have been postulated. Defense compounds indole glucosinolates are synthesized from a derivative of tryptophan, indole-3-acetaldoxime, and may also feed into the auxin pathway. Loss-of-function mutations *wei8 tar2* and *sur2* (red, lower case) disrupt auxin and indole glucosinolate biosynthesis, respectively, and accordingly lead to auxin deficit versus overproduction. Overexpression of *YUC1* also leads to extra auxin being made due to the increased flow through the indole-3-pyruvic acid route, leading to a high-auxin phenotype similar to that of *sur2* null mutants [Color figure can be viewed at wileyonlinelibrary.com]

3.2 | IR-MALDESI sampling development

A. thaliana seedlings proved to be a major challenge for MSI analysis. In order for true biological conclusions to be drawn, there were many steps taken to preserve the biological integrity of samples during IR-MALDESI MSI analysis. These steps are summarized in

Figure 2. Without a new source of moisture, tiny seedlings dry out quickly once they are removed from their growth medium. As such, there needed to be some way to keep them hydrated and alive while allowing for rapid sampling. The moisture issue was solved by sampling specimens from fresh agarose gel that kept them immobilized but moist. It also allowed for decreasing sample analysis time as the curvy seedlings were straightened out when positioned on the surface of the gel, thus requiring a smaller analysis region. In addition, in order to keep the live specimens as fresh as possible, they needed to be kept cool as rising temperatures would result in metabolite changes. However, time constraints and the agarose did not allow for freezing, so the Peltier-cooled stage was kept at around −2°C for the duration of the analysis. The seedlings are also small in diameter, about 50 µm at the smallest dimension. A slight oversampling strategy was employed to ensure that the seedlings were fully ablated and did not slip between the edges of ablation profiles of neighboring laser shots.

There were also challenges associated with analyzing the auxin pathway metabolites. All of the compounds of interest fell in a complex *m/z* space (*m/z* 150–600; Figure S3, supporting information) and were present at low levels, resulting in inconsistent analysis. Due to physical agarose contamination and/or biological variation, abundance values could not be directly compared across or even within genotypes. SIL-IAA was used to solve issues surrounding quantification, and MS/MS was used to ensure the identity of selected ions by comparing their fragmentation patterns with those of standards and literature sources (Figures S4–S6, supporting information).[31]

3.3 | Relative quantification method development

IAA was analyzed for consistency with results obtained using previously established methods of relative quantification.[17] For these methods to be adapted for IAA quantification, four parameters were evaluated relative to previous methods. These were: (1) presence of the metabolite in every scan, (2) mean ion current values consistently above limits of detection, (3) standard deviation, and (4) relative standard deviation (RSD) that was less than 50% and closer to *ca* 30%, as found using previous methods. Ion current is defined here and throughout as the raw intensity values multiplied by IT (IT = 25 ms).[14] Using those parameters, the best concentrations of IAA for stability during laser ablation were 1 and 5 mM, visualized in Figure 3. The optimal concentration of IAA was 1 mM, because it was the lowest concentration that met all requirements, with no additional benefits associated with higher concentrations. However, this concentration is probably four to five orders of magnitude higher than the biologically relevant concentration in wild-type *Arabidopsis* seedlings (*ca* 50–300 nM).[32] When IAA was spiked in at 1 mM, the RSD fell to 23% on average, which was comparable with that of previous relative quantification methods. For concentrations below 100 µM, IAA could not be reliably detected.

In Figure 4, a total of 12 seedlings are shown gently stretched on agarose and analyzed in positive ion mode. SIL-IAA (Figure 4A) is shown to maintain the same ion abundance patterns as off-tissue agarose, demonstrating that it increases with increased agarose sampling (i.e., off-tissue sampling). This was expected, but nonetheless important to illustrate that it could be used to normalize related compounds found in the seedlings. The same abundance trends for total ion current for each scan were also reflected in SIL-IAA (Figure 4B). This provides metabolite normalization for inter-sample (between samples) variability.[33–35] By reflecting intra-sample (within one sample) technical variability, SIL-IAA doped into agarose can be a viable intra-sample and inter-sample quantification compound. Inter-sample relative quantification can be achieved

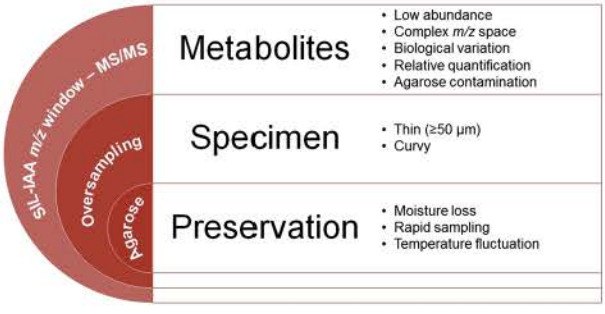

FIGURE 2 Practical concerns in seedling analysis with proposed solutions listed in the red semicircles. Oversampling, dimensions of analysis, and agarose doping steps are further illustrated elsewhere (Figures S7 and S8, supporting information) [Color figure can be viewed at wileyonlinelibrary.com]

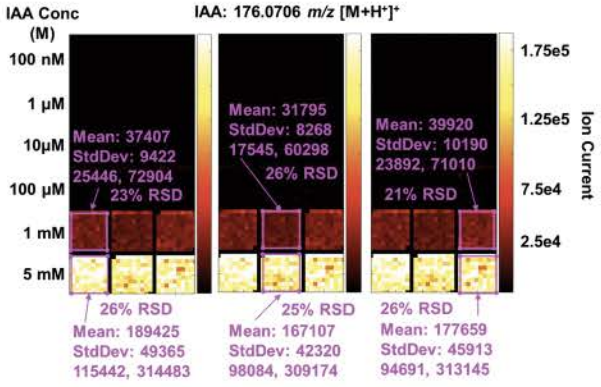

FIGURE 3 Variability characteristics of IAA doped into agarose gel (Figure S7, supporting information). Three replicate 100-voxel squares were analyzed in different locations of each gel made at the IAA concentration listed on the left. The purple boxes highlight those voxels as the basis for statistical analysis. Mean, standard deviation (StdDev), RSD, and range (*X*, *Y*) were recorded for each concentration listed on the side of the image. Each concentration is imaged on the same ion current scale. At 100 nM and 1 µM, IAA was undetectable (ion current: 0). From 10 µM to 100 µM, the ion current was low: 0–1200 and not stable (RSD: 318–1603%). However, at both 1 mM and 5 mM, the IAA signal was consistent with characteristics of SIL compounds sprayed on slides beneath tissues [Color figure can be viewed at wileyonlinelibrary.com]

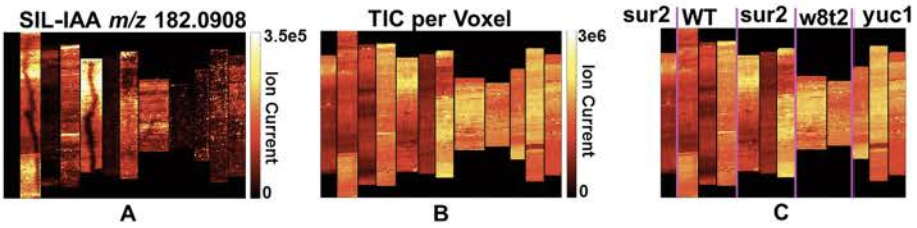

FIGURE 4 Ion abundance of SIL-IAA and agarose. A, SIL-IAA has the same ion abundance patterns with off-tissue agarose. B, The technical variability within each run by plotting the total ion current (TIC) for each voxel. C, The samples analyzed. From left (1) to right (12): 1, *sur2* – control; 2, WT – SIL; 3, WT – SIL; 4, WT – SIL; 5, *sur2* – SIL; 6, *sur2* – SIL; 7, *sur2* – SIL; 8, *wei8 tar2* – SIL; 9, *wei8 tar2* – SIL; 10, *YUC1* ox – SIL; 11, *YUC1* ox – SIL; 12, *YUC1* ox – SIL [Color figure can be viewed at wileyonlinelibrary.com]

because the same concentration of SIL-IAA is doped into the agarose for each sample. Each of these characteristics is necessary for a rigorous quantification strategy.

Figure 5 shows that the normalization of IAA-related compounds to SIL-IAA effectively serves to enhance the images and to provide relative quantification. Some of the compounds are not related to

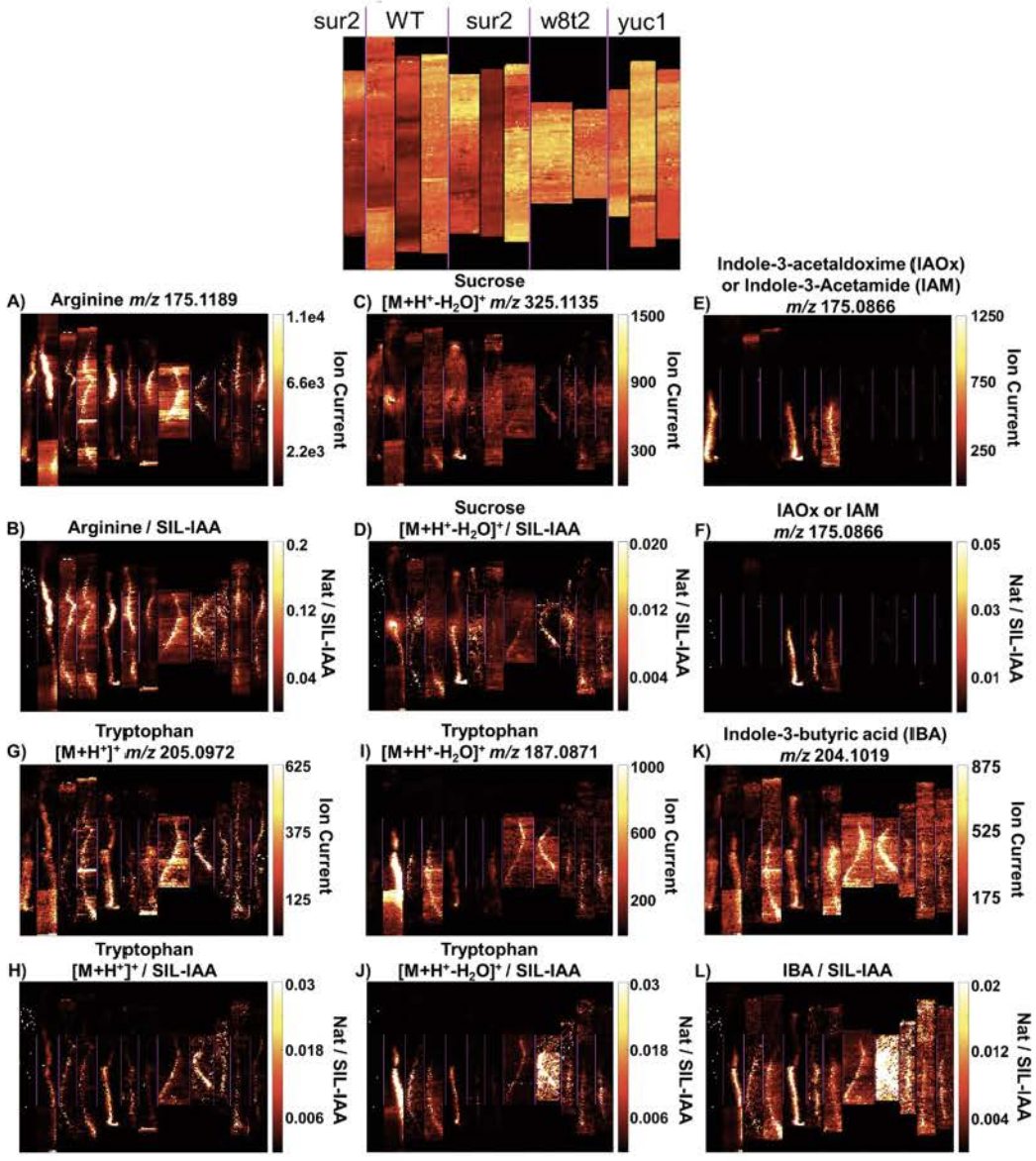

FIGURE 5 Selected images demonstrate analysis of putative plant-produced metabolites that illuminate the seedling (A, B: arginine $[M + H^+]^+$; C, D: sucrose $[M + H^+ - H_2O]^+$) and putative IAA-related metabolites (E, F: IAOx or IAM $[M + H^+]^+$; G, H: tryptophan $[M + H^+]^+$; I, J: tryptophan $[M + H^+ - H_2O]^+$; K, L: indole-3-butyric acid $[M + H^+]^+$). A–D demonstrate the visual improvements made due to normalization and E–L show visual improvements and relative quantification for the molecules similar in structure to SIL-IAA [Color figure can be viewed at wileyonlinelibrary.com]

IAA, and as such the images can be normalized to result in better visualization of the seedlings, but no quantification can be achieved. Several compounds contain similar/identical core structures, which means that both normalization and quantification can be achieved as compounds similar in structure are likely to maintain the same ionization characteristics.[36]

Several IAA- and tryptophan-related metabolites were analyzed and quantified. We were able to distinguish between WT and *sur2* seedlings based on the IAOx/IAM abundances being much higher in *sur2* than in WT, consistent with the defect of this mutant in metabolizing IAOx (Figure 1) and in agreement with a previous report on the *sur2* knockout demonstrating three-orders-of-magnitude higher accumulation of IAOx than wild-type plants.[32] In contrast, IBA, Trp, and Arg did not demonstrate significant differences between mutants and WT.

4 | CONCLUSIONS

A new method of relative quantification for the IR-MALDESI MSI of plants has been developed. Its performance was comparable with those of previously vetted methods of relative quantification used in the analysis of other sample types. In summary, agarose gel was demonstrated to be an appropriate sampling substrate for live plant specimens that must be kept moist and immobilized during analysis using IR-MALDESI. Furthermore, SIL-IAA was doped into the agarose gel and provided quantification by off-tissue normalization. Using this quantification strategy, *sur2* mutant and WT seedlings of *Arabidopsis thaliana* were distinguished in their accumulation of IAOx normalized to SIL-IAA. Future MSI studies of live plant tissues can now rely on this method for metabolite quantification without sacrificing the biological integrity of tissue samples.

ACKNOWLEDGEMENTS

All mass spectrometry measurements were made in the Molecular Education, Technology, and Research Innovation Center (METRIC) at North Carolina State University. This study received financial assistance from the National Institutes of Health grants R01GM087964 (MCB, ME, DM), T32 Biotechnology Traineeship T32GM008776 (MCB), and National Science Foundation grants 1650139, 1444561, and 1750006 (ANS, JMA).

ORCID

David C. Muddiman https://orcid.org/0000-0003-2216-499X

REFERENCES

1. McDonnell LA, Heeren RAM. Imaging mass spectrometry. *Mass Spectrom Rev*. 2007;26(4):606-643. https://doi.org/10.1002/mas.20124
2. Caprioli RM, Farmer TB, Gile J. Molecular imaging of biological samples: Localization of peptides and proteins using MALDI-TOF MS. *Anal Chem*. 1997;69(23):4751-4760. https://doi.org/10.1021/ac970888i
3. Römpp A, Spengler B. Mass spectrometry imaging with high resolution in mass and space. *Histochem Cell Biol*. 2013;139(6):759-783. https://doi.org/10.1007/s00418-013-1097-6
4. Laiko VV, Baldwin MA, Burlingame AL. Atmospheric pressure matrix-assisted laser desorption/ionization mass spectrometry. *Anal Chem*. 2000;72(4):652-657. https://doi.org/10.1021/ac990998k
5. Bergman N, Shevchenko D, Bergquist J. Approaches for the analysis of low molecular weight compounds with laser desorption/ionization techniques and mass spectrometry. *Anal Bioanal Chem*. 2014;406(1):49-61. https://doi.org/10.1007/s00216-013-7471-3
6. Fenn JB, Mann M, Meng CK, Wong SF, Whitehouse CM. Electrospray ionization for mass spectrometry of large biomolecules. *Science*. 1989;246(4926):64-71.
7. Feng R, Konishi Y. Analysis of antibodies and other large glycoproteins in the mass range of 150,000-200,000 daltons by electrospray ionization mass spectrometry. *Anal Chem*. 1992;64(18):2090-2095. https://doi.org/10.1021/ac00042a012
8. Dunn WB, Bailey NJC, Johnson HE. Measuring the metabolome: Current analytical technologies. *Analyst*. 2005;130(5):606-625. https://doi.org/10.1039/B418288J
9. Takáts Z, Wiseman JM, Gologan B, Cooks RG. Mass spectrometry sampling under ambient conditions with desorption electrospray ionization. *Science*. 2004;306(5695):471-473. https://doi.org/10.1126/science.1104404
10. Sampson JS, Hawkridge AM, Muddiman DC. Generation and detection of multiply-charged peptides and proteins by matrix-assisted laser desorption electrospray ionization (MALDESI) Fourier transform ion cyclotron resonance mass spectrometry. *J Am Soc Mass Spectrom*. 2006;17(12):1712-1716. https://doi.org/10.1016/j.jasms.2006.08.003
11. Sampson JS, Murray KK, Muddiman DC. Intact and top-down characterization of biomolecules and direct analysis using infrared matrix-assisted laser desorption electrospray ionization coupled to FT-ICR mass spectrometry. *J Am Soc Mass Spectrom*. 2009;20(4):667-673. https://doi.org/10.1016/j.jasms.2008.12.003
12. Schober Y, Guenther S, Spengler B, Römpp A. Single cell matrix-assisted laser desorption/ionization mass spectrometry imaging. *Anal Chem*. 2012;84(15):6293-6297. https://doi.org/10.1021/ac301337h
13. Robichaud G, Barry JA, Muddiman DC. IR-MALDESI mass spectrometry imaging of biological tissue sections using ice as a matrix. *J Am Soc Mass Spectrom*. 2014;25(3):319-328. https://doi.org/10.1007/s13361-013-0787-6
14. Ekelöf M, Muddiman DC. IR-MALDESI method optimization based on time-resolved measurement of ion yields. *Anal Bioanal Chem*. 2018;410(3):963-970. https://doi.org/10.1007/s00216-017-0585-2
15. Barry JA, Muddiman DC. Global optimization of the infrared matrix-assisted laser desorption electrospray ionization (IR MALDESI) source for mass spectrometry using statistical design of experiments. *Rapid Commun Mass Spectrom*. 2011;25(23):3527-3536. https://doi.org/10.1002/rcm.5262
16. Rosen EP, Bokhart MT, Nazari M, Muddiman DC. Influence of C-trap ion accumulation time on the detectability of analytes in IR-MALDESI MSI. *Anal Chem*. 2015;87(20):10483-10490. https://doi.org/10.1021/acs.analchem.5b02641
17. Bokhart MT, Rosen E, Thompson C, Sykes C, Kashuba ADM, Muddiman DC. Quantitative mass spectrometry imaging of emtricitabine in cervical tissue model using infrared matrix-assisted laser desorption electrospray ionization. *Anal Bioanal Chem*. 2015;407(8):2073-2084. https://doi.org/10.1007/s00216-014-8220-y
18. Dong Y, Li B, Malitsky S, et al. Sample preparation for mass spectrometry imaging of plant tissues: A review. *Front Plant Sci*. 2016;7(60):1–16.

19. Judd R, Bagley MC, Li M, et al. Artemisinin biosynthesis in non-glandular trichome cells of *Artemisia annua*. *Mol Plant*. 2019;12(5):704-714. https://doi.org/10.1016/j.molp.2019.02.011
20. Fideler J, Johanningsmeier SD, Ekelöf M, Muddiman DC. Discovery and quantification of bioactive peptides in fermented cucumber by direct analysis IR-MALDESI mass spectrometry and LC-QQQ-MS. *Food Chem*. 2019;271:715-723. https://doi.org/10.1016/j.foodchem.2018.07.187
21. Ekelöf M, McMurtrie E, Nazari M, Johanningsmeier S, Muddiman D. Direct analysis of triterpenes from high-salt fermented cucumbers using infrared matrix-assisted laser desorption electrospray ionization (IR-MALDESI). *J Am Soc Mass Spectrom*. 2017;28(2):370-375. https://doi.org/10.1007/s13361-016-1541-7
22. Thompson CG, Rosen EP, Prince HMA, et al. Heterogeneous antiretroviral drug distribution and HIV/SHIV detection in the gut of three species. *Sci Transl Med*. 2019;11(499):1–13, eaap8758. https://doi.org/10.1126/scitranslmed.aap8758
23. Stepanova AN, Hoyt JM, Hamilton AA, Alonso JM. A link between ethylene and auxin uncovered by the characterization of two root-specific ethylene-insensitive mutants in Arabidopsis. *Plant Cell*. 2005;17(8):2230-2242. https://doi.org/10.1105/tpc.105.033365
24. Stepanova AN, Robertson-Hoyt J, Yun J, et al. TAA1-mediated auxin biosynthesis is essential for hormone crosstalk and plant development. *Cell*. 2008;133(1):177-191. https://doi.org/10.1016/j.cell.2008.01.047
25. Zhao Y, Christensen SK, Fankhauser C, et al. A role for flavin monooxygenase-like enzymes in auxin biosynthesis. *Science*. 2001;291(5502):306-309. https://doi.org/10.1126/science.291.5502.306
26. Chambers MC, Maclean B, Burke R, et al. A cross-platform toolkit for mass spectrometry and proteomics. *Nat Biotechnol*. 2012;30(10):918-920.
27. Kessner D, Chambers M, Burke R, Agus D, Mallick P. ProteoWizard: Open source software for rapid proteomics tools development. *Bioinformatics*. 2008;24(21):2534-2536. https://doi.org/10.1093/bioinformatics/btn323
28. Race AM, Styles IB, Bunch J. Inclusive sharing of mass spectrometry imaging data requires a converter for all. *J Proteomics*. Special Issue: Imaging Mass Spectrometry: A User's Guide to a New Technique for Biological and Biomedical Research. 2012;75(16):5111-5112. https://doi.org/10.1016/j.jprot.2012.05.035
29. Robichaud G, Garrard KP, Barry JA, Muddiman DC. MSiReader: An open-source interface to view and analyze high resolving power MS imaging files on Matlab platform. *J Am Soc Mass Spectrom*. 2013;24(5):718-721. https://doi.org/10.1007/s13361-013-0607-z
30. Bokhart MT, Nazari M, Garrard KP, Muddiman DC. MSiReader v1.0: Evolving open-source mass spectrometry imaging software for targeted and untargeted analyses. *J Am Soc Mass Spectrom*. 2018;29(1):8-16. https://doi.org/10.1007/s13361-017-1809-6
31. Ozaki T, Nishiyama M, Kuzuyama T. Novel tryptophan metabolism by a potential gene cluster that is widely distributed among Actinomycetes. *J Biol Chem*. 2013;288(14):9946-9956. https://doi.org/10.1074/jbc.M112.436451
32. Novák O, Hényková E, Sairanen I, Kowalczyk M, Pospíšil T, Ljung K. Tissue-specific profiling of the *Arabidopsis thaliana* auxin metabolome. *Plant J*. 2012;72(3):523-536. https://doi.org/10.1111/j.1365-313X.2012.05085.x
33. Cohen LH, Gusev AI. Small molecule analysis by MALDI mass spectrometry. *Anal Bioanal Chem*. 2002;373(7):571-586. https://doi.org/10.1007/s00216-002-1321-z
34. Pirman DA, Kiss A, Heeren RMA, Yost RA. Identifying tissue-specific signal variation in MALDI mass spectrometric imaging by use of an internal standard. *Anal Chem*. 2013;85(2):1090-1096. https://doi.org/10.1021/ac3029618
35. Pirman DA, Reich RF, Kiss A, Heeren RMA, Yost RA. Quantitative MALDI tandem mass spectrometric imaging of cocaine from brain tissue with a deuterated internal standard. *Anal Chem*. 2013;85(2):1081-1089. https://doi.org/10.1021/ac302960j
36. Stokvis E, Rosing H, Beijnen JH. Stable isotopically labeled internal standards in quantitative bioanalysis using liquid chromatography/mass spectrometry: Necessity or not? *Rapid Commun Mass Spectrom*. 2005;19(3):401-407. https://doi.org/10.1002/rcm.1790

SUPPORTING INFORMATION

Additional supporting information may be found online in the Supporting Information section at the end of the article.

How to cite this article: Bagley MC, Stepanova AN, Ekelöf M, Alonso JM, Muddiman DC. Development of a relative quantification method for infrared matrix-assisted laser desorption electrospray ionization mass spectrometry imaging of *Arabidopsis* seedlings. *Rapid Commun Mass Spectrom*. 2020;34:e8616. https://doi.org/10.1002/rcm.8616